Local Atlas-based Adaptive Fiber Tracking

Jan Klein[1], Monique Meuschke[1], Benjamin Geisler[1], and Horst K. Hahn[1]

Fraunhofer MEVIS — Institute for Medical Image Computing, Bremen, Germany,
{jan.klein,monique.meuschke,benjamin.geisler,horst.hahn}@mevis.fraunhofer.de

Abstract. For the MICCAI 2013 DTI tractography challenge we propose a new fiber tracking algorithm which adapts its control parameters locally using a white matter atlas. This allows for a very time efficient reconstruction of fiber bundles whose geometric properties and whose corresponding underlying diffusion processes vary throughout passing brain regions. The basis of our new approach is a conventional deflection-based fiber tracking algorithm which changes its parameters based on an atlas consisting out of 176 regions. Our results show that the corticospinal tract in its entity can be tracked reliably for the given data sets.

1 Introduction

The 2013 DTI tractography challenge aims at evaluating the performances of different fiber tracking algorithms on pre-operative and post-operative diffusion MRI data. The main fiber structure to be reconstructed in the challenge is the corticospinal tract, a large bundle which originates in the precentral gyrus and terminates in the spinal cord. The anatomy of this bundle is well-understood and landmarks like the internal capsule and the cerebral peduncle indicate where this structure has to pass. However, the past two MICCAI challenges have shown that, although using advanced diffusion models and fiber tracking approaches, this large and prominent bundle is still difficult to determine without having false negatives or positives.

We believe that this is mainly due to two reasons: the first reason is that the seeding and filtering of tracked fiber bundles is very important. If having a seed-based approach, placing seed ROIs in the capsula interna or brain stem will not lead to the full corticospinal tract as demonstrated by a large number of papers, e.g., [1–4]. If having a global approach that does not need seed points, the ROIs for filtering are very crucial for the result.

The second reason is that virtually all fiber tracking algorithms depend on several parameters which control the tracking process. Depending on the type of algorithm (deterministic [5, 6] or probabilistic [7], local or global optimization [8, 9]) the parameters may differ. However, in most cases, parameters are assumed to be constant throughout the brain.

As a consequence, fiber bundles are difficult to reconstruct

- if seed ROIs or filter ROIs are not placed properly,
- if the fibers have different geometric properties/shapes in different regions, and
- if the underlying diffusion process is different along the tracts, e.g., if there are kissing or crossing fibers.

Mostly, the modelling of the underlying diffusion process and the development of probabilistic or global approaches is assumed to be the single solution for both problems. However, with this paper we would like to show that there is an alternative approach which uses only diffusion tensors and a deflection-based fiber tracking algorithm. The idea is simple, but very effective: different diffusion processes and geometric properties of fibers require an algorithm whose parameters dynamically adapt to the local situation and do not make any prior assumptions about a global assignment of parameters. Compared to other tracking approaches, the algorithm is easy to understand and to implement, very time-efficient, and produces only few false positives or negatives.

2 Materials and Method

2.1 Image Acquisition

Diffusion weighted image (DWI) data of two patients has been provided, both suffering from tumors in the near vicinity of the corticospinal tract. The patients were scanned using the 3T MRI scanner of the "Advanced Multimodality Image Guided Operating" (AMIGO) suite which is the clinical translational test bed of the National Center for Image-Guided Therapy (NCIGT) at the Brigham and Women's Hospital (BWH) and Harvard Medical School. The data has been acquired using an anisotropic image resolution ($1.146 \times 1.146 \times 5.2$), a repetition number of four to allow for improving the SNR, and a b-value of $1000 s/mm^2$. Additionally, T1-weighted image data (only for patient 1) and FLAIR data were provided.

2.2 Image processing

After motion correction and averaging of the four repetitions, we propose to perform a supersampling of the data before fiber tracking to an isotropic target voxel size using a higher-order filter. This supersampling does not add information to the image, but allows for using a simple tri-linear interpolation at the later tracking stage. As proposed in [10], we use a Lanczos-3 filter in the spatial domain that represents a good trade-off between computational speed and filtering accuracy. In addition to spatial resampling, we smoothed the data using a Gaussian filter. Finally, we computed the diffusion tensors using the Stejskal-Tanner equation.

2.3 Segmentation of the precentral gyrus

Our fiber tracking algorithms needs seed points for the tracking process of the corticospinal tract. It has already been shown, that a whole brain fiber tracking (discrete seed points throughout the brain) leads to better results than using small seed ROIs [11]. However, the disadvantage of a whole brain fiber tracking is its computational effort. Especially, in our case, where we would like to use multiple parameter settings per region, a whole brain seeding strategy would lead to a slow tracking approach. As a consequence, we propose to utilize the whole

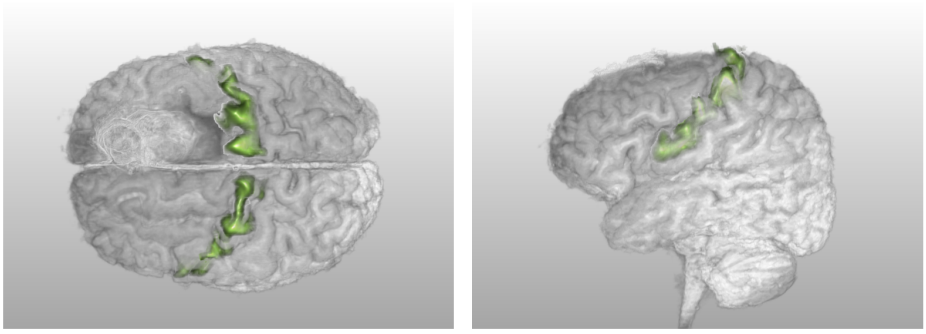

Fig. 1. The precentral gyrus has been segmented using the FA map and is rendered together with the T1 skull-stripped data.

precentral gyrus a seed volume for reconstructing the corticospinal tract. Using an FA map, the segmentation of the precentral gyrus can be done very efficiently by an interactive watershed transformation approach [12]. The same watershed approach can be applied to the T1-weighted image data for the purpose of skull stripping in order to verify the result on the brain surface, see also Figure 1.

2.4 The basic fiber tracking algorithm

The basis of our local, adaptive fiber tracking algorithm is an advection-diffusion based algorithm, which is integrated into NeuroQLab, a software assistant for the purpose of neurosurgical planning and quantitative image analysis [13]. This algorithm, however, could be replaced by virtually any other fiber tracking algorithm and diffusion model. We decided to use this algorithm because it is very time efficient and because it has been ranked as the best algorithm in a clinical study, where the accuracy of nine different tractography algorithms has been examined [14]. In the study, three examiners (neuroradiologist, MRI physicist, and a neurosurgeon) have been double-blinded with respect to the scanned subject (11 men, 9 women) and the fiber tracking algorithm used. They were instructed to evaluate fiber tracking results based on anatomical accuracy of the course of displayed fibers and the number of fibers displayed outside the anatomical boundaries.

Now, our algorithm can be described as follows: for a given tracking position r^t and step length Δs, the next position r^{t+1} is given by

$$r^{t+1} = r^t + \mathbf{d}^t\,\Delta s + \frac{1}{2}\mathbf{k}^t\,\Delta s^2\,.$$

$\mathbf{d}^t$ is computed by using the previous tracking direction $\mathbf{d}^{t-1}$

$$\mathbf{d}' = \left[\alpha \mathbf{v}\mathbf{v}^t + (1-\alpha)\frac{\mathbf{D}}{\lambda_{\max}}\right]\mathbf{d}^{t-1}\,, \qquad \mathbf{d}^t = \frac{\mathbf{d}'}{\|\mathbf{d}'\|}$$

Here, $\mathbf{D}$ is the tensor at $\mathbf{r}^t$ with largest eigenvalue $\lambda_{\max}$ and corresponding eigenvector $\mathbf{v}$; the weight $\alpha \in [0,1]$ interpolates between streamline ($\alpha = 1$) and

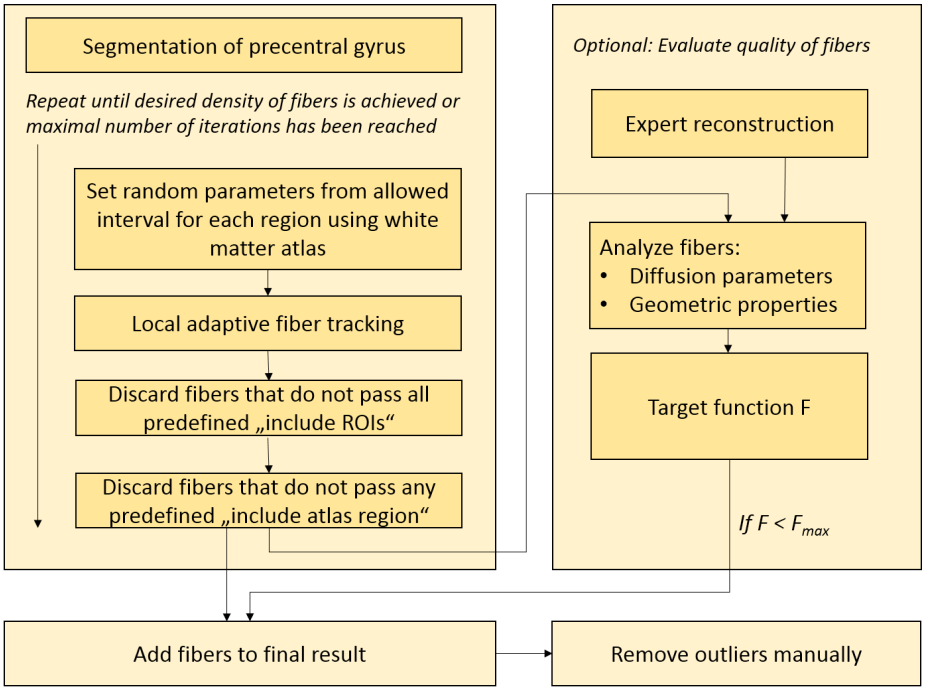

Fig. 2. Algorithmic overview of our proposed method. After each tracking step, the fibers are either directly added to the result or the fibers are evaluated based on an expert reconstruction before.

deflection ($\alpha = 0$) based tracking. Further, $\mathbf{k}^t$ is a curvature term given by

$$\mathbf{k}^t = \frac{\mathbf{d}^t - \mathbf{d}^{t-1}}{\Delta s}$$

which helps improve fiber tracking accuracy. Although we employ this specific basic fiber tracking algorithm in this work, the presented approach and related conclusions can be generalized to other tractography algorithms.

2.5 Atlas-based Parameter Adaption

In addition to the basic algorithm explained in the previous subsection, our new algorithm adapts its control parameters to specific regions of a white matter atlas. For that purpose, we evaluated two different atlases. The first atlas "Colin 27 Average Brain" atlas is based on the T1-MRI data of one healthy volunteer, who has been scanned 27 times within 3 month. From those data an atlas with 50 regions has been generated [15]. The second "JHU-MNI-ss atlas", which is often called "Eve Atlas" [16, 17] is based on the T1-MRI data of 152 healthy volunteers and consists of 176 regions. As the first atlas is relatively coarse and has a region, which covers almost the whole corticospinal tract, we decided to use the JHU-MNI-ss atlas for adapting the following control parameters:

– window length (mm): length of a window where parameters like curvature and FA are averaged. The averaged values are used for comparing with the minimal allowed FA or the maximal allowed curvature instead of comparing the current values directly. As a consequence, local outliers do not immediately stop the tracking process.
– minimal FA value.
– maximal curvature.
– step width (mm): the step width between two consecutive fiber points.

For each tracking position, the corresponding atlas region is determined. If the tracking is reaching a new region, the parameters are randomly changed from predefined intervals, and thus, the reconstruction is locally adapted. The selection is done randomly in order to avoid missing fibers resulting from discrete samplings. Afterwards, it is tested if one of the stopping criteria is reached and if the tracking process should be aborted. If the fibers are determined for all seed points, the tracking process is repeated until a predefined fiber density is reached or the number of iterations exceeds a predefined threshold.

2.6 Assessing the quality and restricting the resulting fibers

As mentioned, the parameters for controlling and influencing the tracking process are chosen randomly from a reasonable range of values. For restricting the range of valid parameters and for an automatic evaluation of the tracked fibers, we developed a tool for manually defining fibers by an expert. The tool allows for placing supporting points of a center line, from which afterwards the fibers are artificially generated. There, one has the opportunity to set the radius of the bundle, the number of fibers, and a jitter factor which randomly deforms the individual fibers. Finally, the fibers can be cropped against an FA map.

This "expert reconstruction" is used afterwards for assessing the tracked fibers. The comparison to the expert reconstruction is done by using diffusion parameters and geometric properties of the fibers. As diffusion parameters, the FA, the ADC, the axial diffusivity and the radial diffusivity is used. For each region, those parameters are determined for the tracked fibers. As these parameters might be similar for geometrically different fiber tracts, we additionally use the Hausdorff distance between the expert reconstruction and the reconstructed fibers, the normalized number of fiber points, and the normalized number of end points to evaluate the tracking result. All these parameters can be combined by a single target function F, which can weight the single parameters individually.

3 Results

The task of the challenge was to submit "the results for the reconstruction of the left and right corticospinal tracts and peritumoral white matter anatomy in two neurosurgical cases". As the definition of "peritumoral" is very imprecise from a mathematical point of view and does not allow for any meaningful comparison of the fiber tracking results, we decided to reconstruct only the left and right corticospinal tract for both patients and visualized the peritumoral white matter anatomy by the given T1 and FLAIR images.

Patient 1, healthy hemisphere	Window length	Min FA	Max curvature	Step width
Precentral gyrus left	[3.24, 4.85]	[0.06, 0.33]	[0.05, 0.48]	[2.99, 4.94]
Corticospinal tract left	[2.71, 4.67]	[0.03, 0.43]	[0.27, 0.65]	[1.36, 5.5]
Cerebral peduncle left	[1.95, 5.61]	[0.03, 0.38]	[0.22, 0.58]	[1.15, 6.23]
Posterior limb of internal capsule left	[1.61, 4.35]	[0.06, 0.4]	[0.41, 0.65]	[1.18, 2.79]
Superior longitudinal fasciculus left	[1.9, 6.0]	[0.11, 0.36]	[0.44, 0.64]	[2.12, 6.68]

Patient 1, diseased hemisphere	Window length	Min FA	Max curvature	Step width
Precentral gyrus right	[1.58, 5.54]	[0.04, 0.43]	[0.24, 0.6]	[0.98, 6.66]
Corticospinal tract right	[3.06, 5.28]	[0.34, 0.43]	[0.25, 0.65]	[2.16, 4.91]
Cerebral peduncle right	[4.16, 5.75]	[0.14, 0.45]	[0.24, 0.64]	[3.18, 6.19]
Posterior limb of internal capsule right	[2.59, 5.66]	[0.13, 0.41]	[0.22, 0.65]	[2.86, 3.42]
Superior longitudinal fasciculus right	[1.73, 5.71]	[0.17, 0.38]	[0.29, 0.48]	[1.24, 5.14]

Fig. 3. The table shows the intervals of some example parameters which were used for computing the corticospinal tract of patient 1. For reconstructing fibers in the diseased hemisphere, the ranges of the intervals are often larger compared to the intervals used for fiber tracking in the healthy hemisphere.

All algorithms have been implemented in MeVisLab using C++. The computations have been performed on an Intel Core i7-2600 with 3.40 GHz and 32 GB main memory. The tracking and filtering process of the corticospinal tract of one hemisphere took around 30 seconds. The most time consuming part is the filtering which is done after each iteration, i.e., if fibers have been tracked for all seed points.

The submitted reconstructed tracts, the videos and the images in Fig. 1 to 9 show the segmented precentral gyrus, the tracked fibers and their proximity to the tumors. It is demonstrated that the fibers end in the precentral gyrus. Furthermore, it can be seen that no false fibers belonging to the corona radiata have been computed. This has been achieved by using seed points only in the precentral gyrus, and not in the capsula interna or in the brain stem as it can be found in many research papers, e.g., see [1–4].

Fig. 3 shows the intervals of parameters for selected areas of the brain. As one can see, for reconstructing fibers in the diseased hemisphere, the used interval ranges are often larger compared to the healthy hemisphere.

4 Discussion and Conclusions

In this paper we have shown that a reliable tracking of the corticospinal tract is possible if adapting the control parameters of the algorithm to the local regions. To the best of our knowledge, this is the first fiber tracking algorithm which adapts its parameters locally using a white matter atlas. Crossing fibers of the corticospinal tract and the superior longitudinal fasicle can easily be determined by our approach if increasing the step width in the corresponding region. Fibers with a high curvature, e.g., fibers of the corticospinal tract ending in "face area" of the precentral gyrus can be computed if increasing the allowed curvature. Note that this parameter adaption can be done fully automatically, also without using the expert reconstruction shown in Section 2.6. In this case, only some more iterations have to be done to get the same quality. Additionally, some more "exclude ROIs" may be needed. The reconstruction of both tracts, left and right, took around one minute on a standard PC.

Future work may examine whether advanced registration techniques can further improve the results. At the moment, only a rigid registration with an allowed scaling is performed. Furthermore, it could be investigated if our approach can benefit from advanced diffusion models like spherical harmonics or Q-ball representations in spite of the given data where a b-value of $1000 s/mm^2$ and a slice thickness of more than 5mm have been selected.

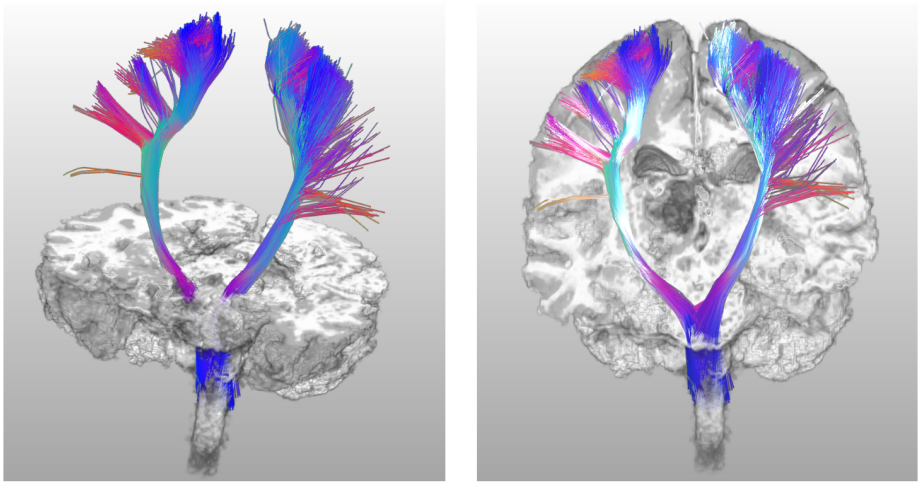

Fig. 4. Patient 1. Tracked fibers of the corticospinal tract with a volume rendering of T1 skull-stripped data.

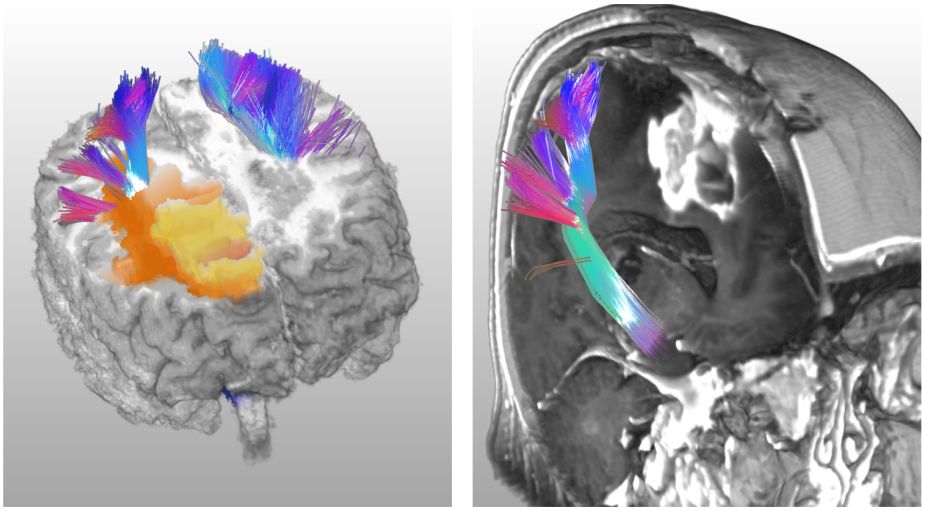

Fig. 5. Patient 1. Fibers and visualized tumor. Especially the left image shows, that only fibers in the precentral gyrus are tracked and not all fibers of the corona radiata. The tumor is visualized in yellow, the edema is shown in orange, and the small part of necrosis is shown in red.

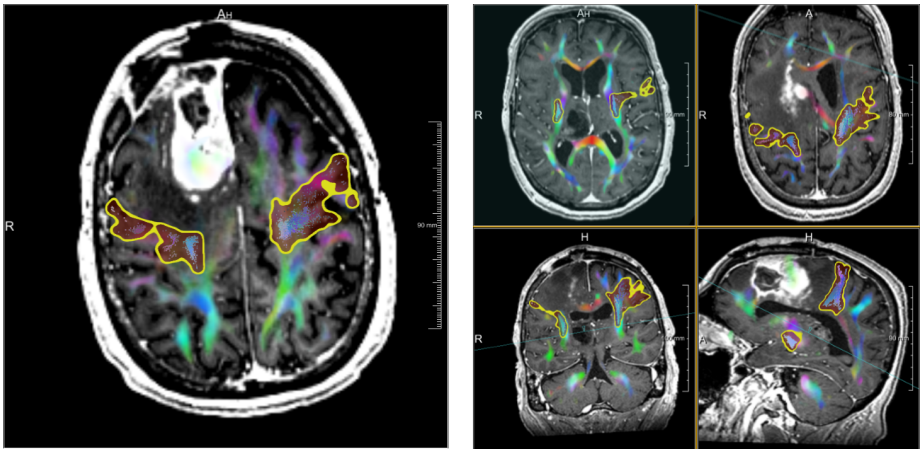

Fig. 6. Patient 1. Fiber tracts are displayed with an additional security margin of 2mm.

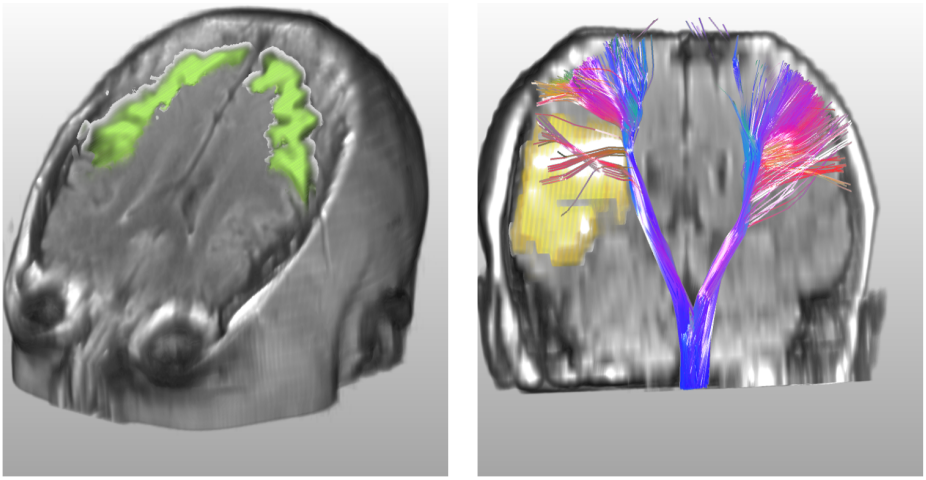

Fig. 7. Patient 2: Left, the segmented precentral gyrus is shown. Due to a missing high-resolution T1 image, only the low-resolution FLAIR image is rendered which does not allow for a proper skull stripping. Right: fibers and visualized tumor.

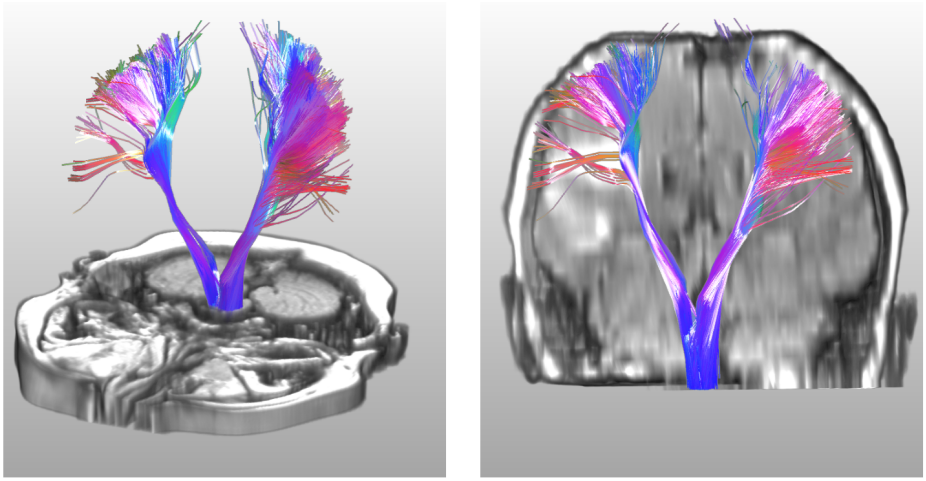

Fig. 8. Patient 2. Tracked fibers with volume rendering of FLAIR data set.

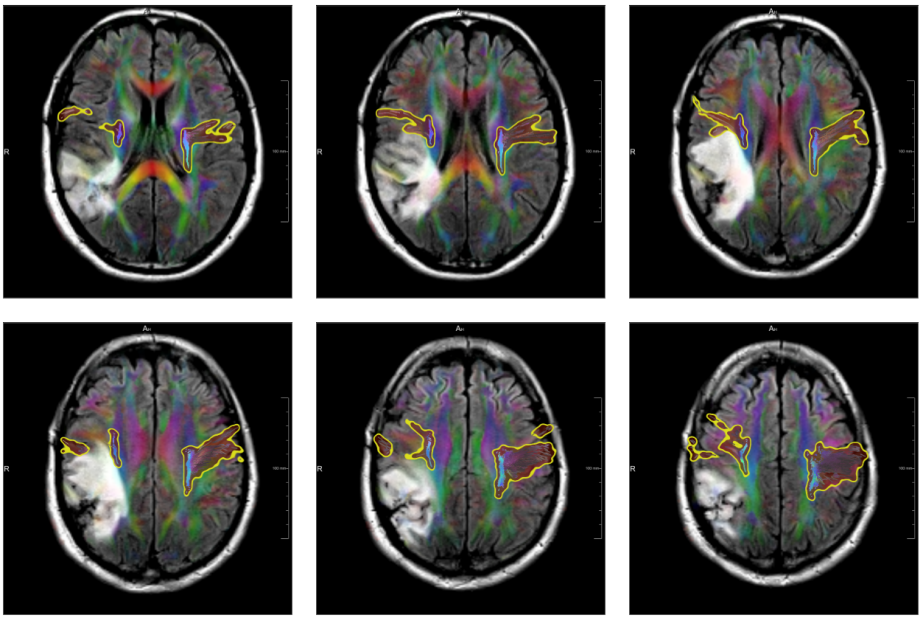

Fig. 9. Patient 2. Fiber tracts are displayed with an additional security margin of 2mm. Different axial slices allow for assessing the proximity of the tracked fibers to the tumor.

References

1. Lee, J.S., Han, M.K., Kim, S.H., Kwon, O.K., Kim, J.H.: Fiber tracking by diffusion tensor imaging in corticospinal tract stroke: Topographical correlation with clinical symptoms. NeuroImage **26**(3) (2005) 771 – 776
2. Niizuma, K., Fujimura, M., Kumabe, T., Higano, S., Tominaga, T.: Surgical treatment of paraventricular cavernous angioma: Fibre tracking for visualizing the corticospinal tract and determining surgical approach. Journal of Clinical Neuroscience **13**(10) (2006) 1028 – 1032
3. Qazi, A.A., Radmanesh, A., O'Donnell, L., Kindlmann, G., Peled, S., Whalen, S., Westin, C.F., Golby, A.J.: Resolving crossings in the corticospinal tract by two-tensor streamline tractography: Method and clinical assessment using fmri. NeuroImage **47, Supplement 2** (2009) T98 – T106
4. Sivaswamy, L., Rajamani, K., Juhasz, C., Maqbool, M., Makki, M., Chugani, H.T.: The corticospinal tract in sturgeweber syndrome: A diffusion tensor tractography study. Brain and Development **30**(7) (2008) 447 – 453
5. Mori, S., Crain, B., Chacko, V., van Zijl, P.: Three-dimensional tracking of axonal projections in the brain by magnetic resonance imaging. Ann Neurol. **45**(2) (1999) 265–269
6. Basser, P., Pajevic, S., Pierpaoli, C., Duda, J., Aldroubi, A.: In vivo fiber tractography using dt-mri data. Magn Reson Med. **44**(4) (2000) 625–632
7. Friman, O., Farnebäck, G., Westin, C.F.: A Bayesian approach for stochastic white matter tractography. IEEE Trans. Medical Imaging **25**(8) (2006) 965–978
8. Fillard, P., Poupon, C., Mangin, J.F.: A Novel Global Tractography Algorithm Based on an Adaptive Spin Glass Model. In: Proceedings of the 12th International

Conference on Medical Image Computing and Computer-Assisted Intervention: Part I. MICCAI '09, Berlin, Heidelberg, Springer-Verlag (2009) 927 – 934
9. Fout, N., Huang, J., Ding, Z.: Visualization of neuronal fiber connections from DT-MRI with global optimization. In: Proceedings of the 2005 ACM symposium on Applied computing. SAC '05, New York, NY, USA, ACM (2005) 1200 – 1206
10. Hahn, H., Klein, J., Nimsky, C., Rexilius, J., Peitgen, H.O.: Uncertainty in diffusion tensor based fiber tracking. Acta Neurochir. Suppl. **98** (2006) 33–41
11. Barbieri, S., Bauer, M.H., Klein, J., Nimsky, C., Hahn, H.K.: Segmentation of fiber tracts based on an accuracy analysis on diffusion tensor software phantoms. NeuroImage **55**(2) (2011) 532 – 544
12. Hahn, H.K.: Morphological Volumetry — Theory, Concepts, and Application to Quantitative Medical Imaging. PhD thesis, University of Bremen (2005)
13. Klein, J., Weiler, F., Barbieri, S., Hirsch, J.G., Geisler, B., Hahn, H.K.: Novel features of neuroqlab - a software assistant for evaluating neuroimaging data. In: Proceedings of European Congress on Radiology (ECR 2012). (2012)
14. Feigl, G.C., Hiergeist, W., Fellner, C., Schebesch, K.M.M., Doenitz, C., Finkenzeller, T., Brawanski, A., Schlaier, J.: Magnetic resonance imaging diffusion tensor tractography: Evaluation of anatomic accuracy of different fiber tracking software packages. World Neurosurgery (2013)
15. Holmes, C., Hoge, R., Collins, L., Woods, R., Toga, A., Evans, A.: Enhancement of mr images using registration for signal averaging. Computer Assisted Tomography **22**(2) (1998) 324–333
16. Mori, S., Oishi, K., Jiang, H., Jiang, L., Li, X., Akhter, K., Hua, K., Faria, A.V., Mahmood, A., Woods, R., Toga, A.W., Pike, G.B., Neto, P.R., Evans, A., Zhang, J., Huang, H., Miller, M.I., van Zijl, P., Mazziotta, J.: Stereotaxic white matter atlas based on diffusion tensor imaging in an ICBM template. NeuroImage **40**(2) (2008) 570–582
17. Oishi, K., Zilles, K., Amunts, K., Faria, A., Jiang, H., Li, X., Akhter, K., Hua, K., Woods, R., Toga, A.W., Pike, G.B., Rosa, P., Evans, A., Zhang, J., Huang, H., Miller, M.I., Van, P.C.M., Mazziotta, J., Mori, S.: Human brain white matter atlas: Identification and assignment of common anatomical structures in superficial white matter. Neuroimage **43** (2008) 447–457